Circulating L-selectin expressing-T cell subsets correlate with the severity of Foxp3 deficiency autoimmune disease

Yuying Liu[1,3], **Thomas K Hoang**[3], **Ting Wang**[3], **Baokun He**[3], **Dat Q Tran**[1], **Jain Zhou**[2], **Nina Tatevian**[2], and **J Marc Rhoads**[1,3]

[1]Department of Pediatrics Pediatric Research Center, The University of Texas Health Science Center at Houston McGovern Medical School (UT Health), Houston, TX 77030, USA

[2]Department of Pathology and Laboratory Medicine, The University of Texas Health Science Center at Houston McGovern Medical School (UT Health), Houston, TX 77030, USA

[3]Department of Pediatrics Gastroenterology, The University of Texas Health Science Center at Houston McGovern Medical School (UT Health), Houston, TX 77030, USA

Abstract

L-selectin (CD62L) is normally highly expressed in naïve T cells. The expression levels of CD62L have been reported to be decreased on T cells during the inflammatory state. It is currently unknown whether the frequency of CD62L$^+$ T cell subsets in the peripheral blood can be used as a marker to indicate is disease severity during inflammation. Our study evaluated whether circulating CD62L$^+$ T cell subsets correlate with the severity of disease by testing an autoimmune condition of scurfy (sf) mouse associated with multi-organ inflammation due to regulatory T cell deficiency. We observed that scurfy mice spontaneously developed an inflammatory phenotype with a significant decrease in the percentage of CD62L-expressing CD4$^+$ T and CD8$^+$ T cells in the peripheral blood. The percentage of CD62L$^+$CD4$^+$ T and CD62L$^+$CD8$^+$ T cells negatively correlated with disease severity, as determined by the weight of spleen and liver, as well as the mean area of lymphocyte infiltrates in lung and liver. The percentage of CD8$^+$ T cells also correlated directly with these markers of disease severity. To conclude, our results support the concept that circulating CD62L-expressing T cells may be used as markers of disease severity in sf mice which is equivalent to a syndrome characterized by immune dysregulation with polyendocrinopathy, enteropathy, and X-linked inheritance (IPEX syndrome) in humans, or in other autoimmune or inflammatory conditions.

Keywords

IPEX syndrome; scurfy mice; immunodeficiency; L-selectin; regulatory T cell

Address correspondence to: Dr. Yuying Liu, Department of Pediatrics Gastroenterology, The University of Texas Health Science Center at Houston McGovern Medical School (UTHealth), 6431 Fannin Street, MSB. 3.135, Houston, TX 77030, USA. Tel: 713-500-5747; Fax: 713-500- 5775; Yuying.Liu@uth.tmc.edu.

Introduction

L-selectin (CD62L) is a cell surface adhesion molecule, which binds to glycolsylated, fucosylated and sulfated sialylated glycoproteins, including CD34, glycosylation-dependent cell adhesion molecule-1 (Glycam-1), and mucosal vascular address in cell adhesion molecule-1 (MadCAM-1) [1–3]. These interactions mediate the rolling of lymphocytes on activated endothelium at the sites of inflammation and homing of cells to the high endothelial venules (HEV) of peripheral lymphoid tissues [4]. In addition, CD62L expression distinguishes small resting memory CD4^{+} T cells that preferentially respond to "recall antigens" [5]. Naive CD4^{+} T cells utilize CD62L expression to facilitate immune surveillance by programming CD4^{high} T cells. When CD62L^{high} naïve T cells become activated upon antigen encounter, CD62L is down-regulated by shedding from the cell membrane to ~10% of the initial value [6–8]. This correlates with a decreased ability of activated T cells to enter lymph nodes [9, 10].

Regulatory T cells (Tregs) modulate the immune system, maintain tolerance to self-antigens, and abrogate autoimmune disease. Classic Tregs specifically express the transcription factor forkhead box p3 (Foxp3). A loss-of-function mutation in Foxp3 is the direct cause of an autoimmune disease characterized by immune dysregulation, polyendocrinopathy, enteropathy, and X-linked inheritance (IPEX syndrome). IPEX syndrome occurs naturally in humans and has been genetically engineered in mice with the "scurfy" (sf) phenotype [11–13]. Inflammation in the Foxp3-deficient sf mouse evolves aggressively, and death occurs within a few weeks after birth. Disease progression is associated with lymphoid and myeloid hyperplasia and inflammation in multiple organs, including the liver, lung, pancreas, and skin [14–16]. A main mediator of this inflammation is the unrestrained activity of autoreactive CD4^{+} effector T-cells, which infiltrate tissues, send recruitment signals to other inflammatory cells, and ultimately lead to tissue damage [17, 18].

Clinical studies of IPEX patients indicate that the percentage of circulating naive CD4^{+} T cells is extremely low, and effector-memory CD4^{+} T cells, in contrast, are high [19]. CD8^{+} T cell subsets have shown a similar trend compared to controls. Currently, Foxp3 gene analysis and fluorescence activated cell sorter (FACS) analysis of lymphocyte CD phenotyping in combination with clinical features have been used to make diagnoses of IPEX syndrome [20]. However, it is currently unknown whether CD markers, such as down-regulated CD62L on CD4^{+} or CD8^{+} T-cells in the peripheral blood are directly correlated with disease severity. In this study we analyzed the correlation between T cell subsets with CD62L expression and several markers of disease severity in the lung, liver, and spleen of sf mice, a murine model of IPEX.

Materials and methods

Scurfy mice

Animal studies were approved by the Animal Welfare Committee of the University of Texas Health Science Center (UT HSC) at Houston (# HSC-AWC-14-056).

Heterozygous female scurfy B6.Cg-Foxp3sf/J mice were purchased from The Jackson Laboratory (Bar Harbor, ME, USA) and bred with C57BL/6 wild-type (WT) male mice to generate hemizygous male B6.Cg-Foxp3sf/Y (scurfy, SF) offspring (n = 22). C57BL/6 WT male littermates were used as controls (n = 19). All mice were held under specific pathogen-free conditions at the animal facility of the University of Texas Medical School at Houston, TX, USA.

Histological analysis of inflammation in lung and liver

Lungs and livers were obtained from WT and SF mice on day 23 of life; they were fixed and processed by the Cellular and Molecular Morphology Core Lab (the Texas Medical Center Digestive Diseases Center, Houston, TX) and stained with hematoxylin and eosin (H&E) for histological evaluation. Lung Injury Scores (LIS) were recorded by evaluating in histological samples area of alveolar septal thickening and the amount of proteinaceous debris that filled airspaces. Digitized images of stained tissues were taken by using Olympus Bx51 (Pennsylvania, USA) microscope at $100 \times$ magnification. The area of lymphocyte infiltrates was measured by using the software Image J (NIH, USA). Three fields of photomicrographs from each sample were taken to measure 3–5 areas of lymphocyte infiltrates. The mean areas (μm^2) of lymphocyte infiltrates in lung and liver, respectively, for each mouse were calculated to express the severity of inflammation. Spleens were obtained from WT and SF mice on day 23 of life and were weighed to express the severity of the disease.

Plasma cytokine IFN-γ and IL-2 analysis

Plasma samples were collected from SF and WT mice on day 23 of life. Cytokines IFN-γ and IL-2 were assessed by using a mouse MSD V-Plex cytokine assay kit (Meso Scale Discovery, Gaithersburg, MD). The assay was run according to the manufacturer's instructions. The detection ranges from the standard curve of this assay are 0.243–191 pg/mL for IFN-γ; 2.76–517 pg/mL for IL-2.

Lung and liver tissue preparation for IL-1β analysis

Lung and liver tissues were homogenized in 0.4 ml of lysis buffer containing protease inhibitors with 20 mmol/l Tris·HCl (pH 7.5), 150 mmol/l NaCl, 1 mmol/l Na^2 EDTA, 1 mmol/l EGTA, 1% NP-40, 1% sodium deoxycholate, 2.5 mmol/l Na^3VO^4, 1 μg/ml leupeptin, 1 μg/ml aprotinin, and 1 mmol/l PMSF. The homogenates were centrifuged at 14,000 g for 10 min at 4°C after incubation on ice for 30 min. A mouse cytokine kit from MSD was used according to the manufacturer's protocol to measure IL-1β in the collected supernatant. The detection range from the standard curve of this assay is 1.49–360 pg/ml. The protein concentration of tissue lysates was measured by using Bio-Rad Dc Protein Assay (Bio-Rad Laboratories, Hercules, CA) according to the manufacturer's instruction, expressed as mg/mL total protein. Final cytokine levels were normalized by the total protein in the collected supernatant, reported as pg/mg total protein.

Flow cytometry analysis

Whole blood (~100 microliter) was directly surface- stained with the following fluorochrome-conjugated anti-mouse antibodies: (1) CD3 (17A2) conjugated with

fluorescein isothiocyanate (FITC), (2) CD4 (GK1.5) conjugated with peridinin-chlorophyl proteins (PerCP/Cy5.5), (3) CD8a (53–6.7) conjugated with phycoerythrin (PE), and (4) CD62L (MEL-14) conjugated with Allophycocyanin (APC) from Biolegend (San Diego, CA). To confirm the phenotype of scurfy mice, the anti-mouse antibodies FOPX3 (FJK-16a) conjugated with Alexa Fluor 647 (AF647, eBioscience, San Diego, CA) was used for intracellular staining. Fixation and permeabilization were done using afixation/permeabilization kit according to the manufacturer's protocol (eBioscience). Single-cell suspensions from spleens were obtained by gentle fragmentation and filtration of the tissues through 40-μm cell strainers into RPMI 1640 (Sigma) complete medium containing collagenase V (0.1 mg/ml) from Clostridium histolyticum (Sigma, St. Louis, MO). MACS buffer consisting of phosphate buffered saline, 0.5% bovine serum albumin (Hyclone Laboratories), and 2 mM EDTA (Lonza, Bethesda, MD) was used for washing the cells. Finally, cells were resuspended in MACS buffer for surface and intracellular staining using specific antibodies. All samples were analyzed with FACSCalibur (BD Biosciences) and processed with FlowJo (TreeStar, Ashland, OR).

Statistical analysis

Data are expressed as means ± SE. Two-way ANOVA with Bonferroni Posttests was used for group value comparisons. Pearson Correlation was performed and significance was analyzed using Prism (GraphPad Software, San Diego, CA, USA). *P*-values <0.05 were considered significant.

Results

Scurfy mice spontaneously develop an inflammation phenotype

Scurfy mice begin to develop scaly skin on their ears, eyes and tails on day 13 of life (Figure 1A). Around day 23 of life, all scurfy mice but no normal WT males developed pneumonitis (Figure 1B), characterized by alveolar wall thickening, interstitial edema, perivascular and peribronchial lymphocyte infiltrates, as well as focal hemorrhages. Lung injury scores (which takes into consideration the area of filled air-spaces with proteinaceous debris and the area of alveolar septal thickening) were found to be significantly higher in SF compared to WT mice (P<0.001) (Figure 1C). In addition, in the livers of scurfy mice, but not WT mice, we found periportal and perisinusoidal lymphocytic infiltrates (Figure 1D). The plasma levels of inflammatory cytokines IFN-γ and IL-2 (Figure 1E) in scurfy mice were significantly increased compared to their WT counterparts (P<0.001). Inflammatory IL-1β levels were significantly increased in the lung (P<0.05) and liver (P<0.001) tissue lysates (Figure 1F). Focusing on the number of T cells, we observed that the percentages of CD3^{+} T cells in the total lymphocyte population were significantly increased both in the spleen (P<0.001) and among peripheral blood leukocytes (P<0.05) (Figure 1G).

Scurfy mice have decreased circulating CD62L-expressing T cells

We further identified two general T cell subsets: CD4^{+} T cells (T helper cells) and CD8^{+} T cells (cytotoxic T cells) in the blood. CD4^{+} and CD8^{+} T cells were defined as shown in Figure 2A using FACS analysis. Additionally, the percentage of cells expressing CD62L among CD4^{+} T cells or CD8^{+} T cells was analyzed (Figure 2A).

Compared to the WT mice, scurfy mice had a significant increase in the percentage of $CD4^+$ T cells (SF: $25.6 \pm 2.4\%$ vs. WT: $17.9 \pm 0.9\%$, P<0.05) but a significant decrease in the percentage of $CD62L^+CD4^+$ T cells (SF: $33.2 \pm 2.6\%$ vs. WT: $88.3 \pm 1.3\%$, P<0.001) (Figure 2B). In addition, scurfy mice had a significant increase in circulating $CD8^+$ T cells (SF: $29.3 \pm 2.2\%$ vs. WT: $8.6 \pm 0.8\%$, P<0.001). However, $CD62L^+CD8^+$ T cells were reduced in scurfy mice (SF: $25.4 \pm 2.2\%$ vs. WT: $84.5 \pm 2.7\%$, P<0.001) (Figure 2C).

Severity of splenomegaly was associated with a reduction in CD62L$^+$ T cells in SF mice

Spleen weight (in grams, g) was significantly increased in SF compared to WT mice (SF: 0.1142 ± 0.0096 g vs. WT: 0.0504 ± 0.0037 g. P<0.0001) (Figure 3A). This increase could be an index of the severity of the disease. To evaluate whether CD62L as an immune cell marker in the peripheral blood could reflect severity of disease, we questioned if there was a correlation between $CD62L^+$ T cells and splenic weight. Our results indicated that the % of $CD62L^+CD4^+$ T cells was negatively correlated with spleen weight in all mice (WT and SF) (r = −0.7826, P<0.0001). We identified two separate clusters of CD62L cells: WT (with a higher % of $CD62L^+CD4^+$ T cells) and SF (with lower % of $CD62L^+CD4^+$ T cells) (as shown in the dotted rectangle). More importantly, in the group of SF mice, we also demonstrated a significant negative correlation between the % of $CD62L^+CD4^+$ T cells and spleen weight (r = −0.6010, P = 0.0040) (Figure 3B). When we analyzed $CD8^+$ cells, we observed the same negative correlation between the % of $CD62L^+CD8^+$ T cells and spleen weight. The correlation was significant when we included all mice (WT and SF) (r = −0.6635, P<0.0001) (Figure 3C). Additionally, the % of $CD8^+$ T cells positively correlated with spleen weight (r = 0.7512, P<0.0001), when analyzing data from all animals (WT and SF) (Figure 3D), and when analyzing data from only the SF group (r = 0.5240, P = 0.0148) (Figure 3D in the dotted line rectangle).

CD62L$^+$ T cells negatively correlated with the mean area of lymphocyte infiltrates in lung of SF mice

A prominent abnormality in SF mice was lung inflammation, characterized by perivascular and peribronchial lymphocyte infiltrates (Figure 4A). To evaluate the severity of the disease, we measured the area of lymphocyte infiltrates as indicated in Figure 4A. Subsequently, we calculated the mean area of lymphocyte infiltrates for each SF mouse. It showed a significant increase in the mean area of lymphocyte infiltrates in SF mice compared to WT controls (P<0.0001) (Figure 4B). In addition, a negative correlation of the mean area of lymphocyte infiltrates with the % of $CD62L^+$ T cells was observed. Area of lymphocyte infiltrates correlated negatively with both the % of $CD62L^+CD4^+$T cells (r = −0.4947, P = 0.0226, Figure 4C) and the % of $CD62L^+CD8^+$ T cells (r = −0.5439, P = 0.0132, Figure 4D), while the mean area of lymphocyte infiltrates correlated positively with % of $CD8^+$ T cells in the peripheral blood (r = 0.7276, P = 0.0002, Figure 4E).

CD62L$^+$ T cells negatively correlated with inflammatory changes in liver of SF mice

Scurfy mice exhibited hepatomegaly, with a significantly increased liver weight compared to WT mice (Figure 5A, P = 0.0023). Scurfy mice had evidence of major periportal and perisinusoidal lymphocyte infiltrates in the liver (Figure 1D). The mean area of lymphocyte infiltrate in the liver was significantly increased in SF mice compared to WT controls

(P<0.0001) (Figure 5B). We used the histological specimens to quantify disease severity and observed that the % of peripheral blood $CD62L^+CD4^+$ T cells negatively correlated with liver weight (r = −0.5029, P = 0.0171) (Figure 5C). Furthermore, the mean area of lymphocyte infiltration in liver of SF mice was negatively correlated with the % of circulating $CD62L^+CD4^+$ T cells (r = −0.5733, P = 0.0066) (Figure 5D). As seen in lung tissue, we found a positive correlation between the % of $CD8^+$ T cells and area of periportal lymphocyte infiltration (r = 0.6446, P = 0.0022) (Figure 5E).

Discussion

In this study, we demonstrated a "yin-yang" relationship between circulating $CD62L^+$ T cells and organ infiltration with lymphocytes. We suggest that peripheral blood CD62L loss may represent an inflammation marker indicating the severity of the Treg-deficient autoimmune disease. Currently, autoimmune disease activity is monitored by clinical symptoms and by using nonspecific blood markers such as erythrocyte sedimentation rate (ESR) and C-reactive protein (CRP) level. However, a number of autoimmune conditions are produced by specific mutations in the maturation of T cells, leading to uncontrolled T cell mediated inflammation. Such conditions include the IPEX syndrome studied in the current investigations [21, 22], IPEX-like syndromes due to CD25 deficiency, STAT5b deficiency and STAT1 mutations [23, 24]; and Wiskott-Aldrich syndrome, a very similar condition to IPEX, producing severe dermatitis and splenomegaly with abnormal Treg function [25]. Post-bone marrow transplant graft-versus- host disease (GVHD) also bears similarities to IPEX syndrome [26].

Similar to the practice of monitoring total $CD4^+$ T cell numbers in patients with human immunodeficiency syndrome, $CD62L^+$ cells might be used to monitor disease activity and to gauge the response to pharmacological interventions in children with T-cell mediated autoimmunity and/or immunodeficiency. Such an approach has been undertaken in humans with type 1 diabetes mellitus. Severe depletion of $CD4^+CD25^{hi}CD62L^+$ cells was noted in the circulating blood of these patients when they developed microvascular complications [27]. The transfer of $CD62L^+$ cells into non-obese diabetic mice prevented the onset of diabetes [28]. In experimental autoimmune uveoretinitis, dendritic cells suppressed ocular inflammation via activation of these L-selectin-expressing T cells [29], leading to the hypothesis that IL-10 elaboration by dendritic cells promoted the migration of CD62L-expressing *regulatory* T cells to the site of inflammation.

It is crucial that the immunologically active cells are able to respond to pathogens to maintain health in multicellular organisms. Immune surveillance allows lymphocytes to find their cognate antigens. The lymphocytes must leave circulation and move into secondary lymphoid organs, such as lymph nodes, where antigens are presented. After antigen encounter, a process of guided delivery of immune cells to sites of inflammation orchestrates a healthy host defense. Adhesion molecules such as L-selectin (CD62L), control both constitutive and inflammatory leukocyte trafficking. Studies on L-selectin-deficient mice ($CD62L^{-/-}$) compared to L-selectin-sufficient mice showed (1) lower numbers of circulating lymphocytes, (2) increased memory cell numbers, (3) altered homing profiles of sub-populations of lymphocytes, and (4) impaired T cell proliferation and cytokine production

[4, 30–32]. Therefore, CD62L expressed constitutively on leukocytes, plays a particularly pivotal role in highly dynamic leukocyte-endothelium interactions. CD62L is responsible for constitutive lymphocyte trafficking to lymph nodes, lymphocyte homing to intestinal Peyer's patches, and direct lymphocytes and neutrophil migration into sites of inflammation.

Effector or memory $CD4^+$ T cell and $CD8^+$ T cell homeostasis is critically controlled by Tregs [18, 33]. In scurfy mice and in human IPEX syndrome, the percentage and absolute number of $CD4^+$ and $CD8^+$ T cells with effector/memory phenotype ($CD44^{high}$ or $CD62L^{low}$) was significantly increased [18, 20, 34]. Naïve T cells express high surface levels of L-selectin. After naïve T cells become activated by exposure to an antigen they undergo a transformation. Activated cells rapidly divide and differentiate into L-selectin^{low} effector cells. After successful elimination of the antigen, most T cells undergo apoptosis but some of the cells evolve into memory cells. A variety of stimuli, including T cell receptor engagement, CD3 cross-linking, and protein kinase C activation influence the surface expression of L-selectin *in vivo* and *in vitro*. L-selectin is regulated at transcriptional, translational and proteolytic levels. During the activation of T cells, factors determining surface L-selectin include mRNA expression, mRNA stability, transcription rate and shedding rate [35]. The down-regulation of CD62L that accompanies T lymphocyte activation most often redirects cells away from lymph nodes to sites of inflammation or infection [36]. This concept has recently been challenged by investigators who study transgenic mice in which constitutive CD62L expression is maintained, rather than down-regulated, followed by T cell activation [37]. These latter studies reveal a novel role for CD62L ectodomain proteolysis in promoting rapid and efficient vial clearance.

The correlation of CD62L with inflammation has been studied in human diseases. Recent studies showed that naïve T cells correlate with mucosal healing in patients with inflammatory bowel disease [38], demonstrating that mucosal healing was reflected by almost a 100% increase of CD62L expression in mucosal T cells in patients in remission compared to those with active inflammation. The correlation of CD62L and skin damage in systemic sclerosis has also been studied; results showed a highly significant negative correlation between soluble L-selectin concentration and disease activity and severity [39].

In addition to $CD62L^+$ T cells, we observed that the percentage of total $CD8^+$ T cells in lymphocyte population in peripheral blood was increased in scurfy mice compared to WT mice. We consistently found that the % of $CD8^+$ T cells positively correlated with increased spleen and liver weight and mean area of lymphocyte infiltrates in lung and liver in scurfy mice. An increase in $CD8^+$ T cells has been shown to play a role in progression of the autoimmune process. For example, an increase in the $CD8^+$ lymphocytes expressing perforin and granzyme B was correlated with enhanced disease activity in systemic lupus erythematosus (SLE) patients [40]. A high frequency of IFN-γ^+ $CD8^+$ T cells correlated with disease activity in the presence of autoantibodies. Changes of the numbers and/ or activity of IFN-γ^+ producing $CD8^+$ T cells can therefore explain the phases of flares and remission of SLE disease [40, 41]. Recent studies showed that unique IL-21-producing c-Maf$^+CD4^+$ T cells develop in the absence of Foxp3$^+$ Treg cells, which induce effector $CD8^+$ T cells and enhance multi-organ autoimmune inflammation in sf mice [42]. Further studies determining whether the $CD8^+$ T cells are IFN-γ-producing cells are needed to explore the

cellular mechanisms of autoimmunity in scurfy mice. The positive correlation between % of CD8$^+$ T cells and disease severity indicates that the circulating % of CD8$^+$ T cells may be pathogenetically important and also may serve as a marker of disease severity.

In conclusion, monitoring disease-specific inflammation in diseases such as IPEX syndrome or WAS currently may require exposure to radiation (computerized tomography) or invasive studies, such as liver biopsy, bronchoscopy, or endoscopy. We hypothesize that CD62L$^+$ CD4$^+$ and CD8$^+$ T cells in circulating blood may be studied as an indicator of T cell autoimmune disease activity could be used to monitor response to experimental therapies. Further studies are required to determine and confirm the circulating CD62L$^+$ T cell subsets in human IPEX syndrome or other human autoimmune diseases.

Acknowledgments

References

1. Bargatze RF, Jutila MA, Butcher EC. Distinct roles of L-selectin and integrins alpha 4 beta 7 and LFA-1 in lymphocyte homing to Peyer's patch-HEV in situ: the multistep model confirmed and refined. Immunity. 1995; 3:99–108. [PubMed: 7542550]

2. Kohn LA, Hao QL, Sasidharan R, Parekh C, Ge S, Zhu Y, Mikkola HK, Crooks GM. Lymphoid priming in human bone marrow begins before expression of CD10 with upregulation of L-selectin. Nat Immunol. 2012; 13:963–71. [PubMed: 22941246]

3. Nicholson MW, Barclay AN, Singer MS, Rosen SD, van der Merwe PA. Affinity and kinetic analysis of L-selectin (CD62L) binding to glycosylation- dependent cell-adhesion molecule-1. J Biol Chem. 1998; 273:763–70. [PubMed: 9422729]

4. Steeber DA, Green NE, Sato S, Tedder TF. Lyphocyte migration in L-selectin-deficient mice. Altered subset migration and aging of the immune system. J Immunol. 1996; 157:1096–106. [PubMed: 8757614]

5. Hengel RL, Thaker V, Pavlick MV, Metcalf JA, Dennis G Jr, Yang J, Lempicki RA, Sereti I, Lane HC. Cutting edge: L-selectin (CD62L) expression distinguishes small resting memory CD4+ T cells that preferentially respond to recall antigen. J Immunol. 2003; 170:28–32. [PubMed: 12496379]

6. Bell EB, Westermann J. CD4 memory T cells on trial: immunological memory without a memory T cell. Trends Immunol. 2008; 29:405–11. [PubMed: 18674966]

7. Jung TM, Dailey MO. Rapid modulation of homing receptors (gp90MEL-14) induced by activators of protein kinase C. Receptor shedding due to accelerated proteolytic cleavage at the cell surface. J Immunol. 1990; 144:3130–6. [PubMed: 2182714]

8. Smalley DM, Ley K. L-selectin: mechanisms and physiological significance of ectodomain cleavage. J Cell Mol Med. 2005; 9:255–66. [PubMed: 15963248]

9. Galkina E, Tanousis K, Preece G, Tolaini M, Kioussis D, Florey O, Haskard DO, Tedder TF, Ager A. L-selectin shedding does not regulate constitutive T cell trafficking but controls the migration pathways of antigen-activated T lymphocytes. J Exp Med. 2003; 198:1323–35. [PubMed: 14597735]

10. Venturi GM, Tu L, Kadono T, Khan AI, Fujimoto Y, Oshel P, Bock CB, Miller AS, Albrecht RM, Kubes P, Steeber DA, Tedder TF. Leukocyte migration is regulated by L-selectin endoproteolytic release. Immunity. 2003; 19:713–24. [PubMed: 14614858]

11. Bennett CL, Christie J, Ramsdell F, Brunkow ME, Ferguson PJ, Whitesell L, Kelly TE, Saulsbury FT, Chance PF, Ochs HD. The immune dysregulation, polyendocrinopathy, enteropathy, X-linked

syndrome (IPEX) is caused by mutations of FOXP3. Nat Genet. 2001; 27:20–1. [PubMed: 11137993]

12. Brunkow ME, Jeffery EW, Hjerrild KA, Paeper B, Clark LB, Yasayko SA, Wilkinson JE, Galas D, Ziegler SF, Ramsdell F. Disruption of a new forkhead/winged-helix protein, scurfin, results in the fatal lymphoproliferative disorder of the scurfy mouse. Nat Genet. 2001; 27:68–73. [PubMed: 11138001]

13. Wildin RS, Ramsdell F, Peake J, Faravelli F, Casanova JL, Buist N, Levy-Lahad E, Mazzella M, Goulet O, Perroni L, Bricarelli FD, Byrne G, McEuen M, Proll S, Appleby M, Brunkow ME. X-linked neonatal diabetes mellitus, enteropathy and endocrinopathy syndrome is the human equivalent of mouse scurfy. Nat Genet. 2001; 27:18–20. [PubMed: 11137992]

14. Fontenot JD, Gavin MA, Rudensky AY. Foxp3 programs the development and function of CD4+CD25+ regulatory T cells. Nat Immunol. 2003; 4:330–6. [PubMed: 12612578]

15. Godfrey VL, Wilkinson JE, Russell LB. X-linked lymphoreticular disease in the scurfy (sf) mutant mouse. Am J Pathol. 1991; 138:1379–87. [PubMed: 2053595]

16. Lyon MF, Peters J, Glenister PH, Ball S, Wright E. The scurfy mouse mutant has previously unrecognized hematological abnormalities and resembles Wiskott-Aldrich syndrome. Proc Natl Acad Sci U S A. 1990; 87:2433–7. [PubMed: 2320565]

17. Kanangat S, Blair P, Reddy R, Daheshia M, Godfrey V, Rouse BT, Wilkinson E. Disease in the scurfy (sf) mouse is associated with overexpression of cytokine genes. Eur J Immunol. 1996; 26:161–5. [PubMed: 8566060]

18. Blair PJ, Bultman SJ, Haas JC, Rouse BT, Wilkinson JE, Godfrey VL. CD4+CD8- T cells are the effector cells in disease pathogenesis in the scurfy (sf) mouse. J Immunol. 1994; 153:3764–74. [PubMed: 7930593]

19. Costa-Carvalho BT, de Moraes-Pinto MI, de Almeida LC, de Seixas Alves MT, Maia RP, de Souza RL, Barreto M, Lourenço L, Vicente AM, Coutinho A, Carneiro-Sampaio M. A remarkable depletion of both naive CD4+ and CD8+ with high proportion of memory T cells in an IPEX infant with a FOXP3 mutation in the forkhead domain. Scand J Immunol. 2008; 68:85– 91. [PubMed: 18489537]

20. Zennaro D, Scala E, Pomponi D, Caprini E, Arcelli D, Gambineri E, Russo G, Mari A. Proteomics plus genomics approaches in primary immunodeficiency: the case of immune dysregulation, polyendocrinopathy, enteropathy, X-linked (IPEX) syndrome. Clin Exp Immunol. 2012; 167:120– 8. [PubMed: 22132891]

21. Hannibal, MC., Torgerson, T. IPEX Syndrome. In: Pagon, RA.Adam, MP.Ardinger, HH.Wallace, SE.Amemiya, A.Bean, LJH.Bird, TD.Fong, CT.Mefford, HC.Smith, RJH., Stephens, K., editors. GeneReviews®[Internet]. Seattle (WA): University of Washington, Seattle; 1993–2015.

22. Vasiljevic A, Poreau B, Bouvier R, Lachaux A, Arnoult C, Fauré J, Cordier MP, Ray PF. Immune dysregulation, polyendocrinopathy, enteropathy, X-linked syndrome and recurrent intrauterine fetal death. Lancet. 2015; 385:2120. [PubMed: 26009232]

23. Verbsky JW, Chatila TA. T-regulatory cells in primary immune deficiencies. Curr Opin Allergy Clin Immunol. 2011; 11:539–44. [PubMed: 21986549]

24. Verbsky JW, Chatila TA. Immune dysregulation, polyendocrinopathy, enteropathy, X-linked (IPEX) and IPEX-related disorders: an evolving web of heritable autoimmune diseases. Curr Opin Pediatr. 2013; 25:708–14. [PubMed: 24240290]

25. Massaad MJ, Ramesh N, Geha RS. Wiskott- Aldrich syndrome: a comprehensive review. Ann N Y Acad Sci. 2013; 1285:26–43. [PubMed: 23527602]

26. Pulsipher MA, Wayne AS, Schultz KR. New frontiers in pediatric Allo-SCT: novel approaches for children and adolescents with ALL. Bone Marrow Transplant. 2014; 49:1259–65. [PubMed: 24933210]

27. El-Samahy MH, Adly AA, Ismail EA, Salah NY. Regulatory T cells with CD62L or TNFR2 expression in young type 1 diabetic patients: relation to inflammation, glycemic control and micro-vascular complications. J Diabetes Complications. 2015; 29:120–6. [PubMed: 25113439]

28. You S, Slehoffer G, Barriot S, Bach JF, Chatenoud L. Unique role of CD4+CD62L+ regulatory T cells in the control of autoimmune diabetes in T cell receptor transgenic mice. Proc Natl Acad Sci U S A. 2004; 101(Suppl 2):14580–5. [PubMed: 15340148]

29. Lau AW, Biester S, Cornall RJ, Forrester JV. Lipopolysaccharide-activated IL-10-secreting dendritic cells suppress experimental autoimmune uveoretinitis by MHCII-dependent activation of CD62L-expressing regulatory T cells. J Immunol. 2008; 180:3889–99. [PubMed: 18322197]

30. Arbonés ML, Ord DC, Ley K, Ratech H, Maynard- Curry C, Otten G, Capon DJ, Tedder TF. Lymphocyte homing and leukocyte rolling and migration are impaired in L-selectin-deficient mice. Immunity. 1994; 1:247–60. [PubMed: 7534203]

31. Steeber DA, Tang ML, Zhang XQ, Muller W, Wagner N, Tedder TF. Efficient lymphocyte migration across high endothelial venules of mouse Peyer's patches requires overlapping expression of L-selectin and beta7 integrin. J Immunol. 1998; 161:6638–47. [PubMed: 9862692]

32. Xu J, Grewal IS, Geba GP, Flavell RA. Impaired primary T cell responses in L-selectin-deficient mice. J Exp Med. 1996; 183:589–98. [PubMed: 8627170]

33. Sharma R, Zheng L, Deshmukh US, Jarjour WN, Sung SS, Fu SM, Ju ST. A regulatory T cell-dependent novel function of CD25 (IL-2Ralpha) controlling memory CD8(+) T cell homeostasis. J Immunol. 2007; 178:1251–5. [PubMed: 17237369]

34. Bakke AC, Purtzer MZ, Wildin RS. Prospective immunological profiling in a case of immune dysregulation, polyendocrinopathy, enteropathy, X-linked syndrome (IPEX). Clin Exp Immunol. 2004; 137:373–8. [PubMed: 15270855]

35. Chao CC, Jensen R, Dailey MO. Mechanisms of L-selectin regulation by activated T cells. J Immunol. 1997; 159:1686–94. [PubMed: 9257829]

36. Tedder TF, Steeber DA, Pizcueta P. L-selectindeficient mice have impaired leukocyte recruitment into inflammatory sites. J Exp Med. 1995; 181:2259–64. [PubMed: 7539045]

37. Richards H, Longhi MP, Wright K, Gallimore A, Ager A. CD62L (L-selectin) down-regulation does not affect memory T cell distribution but failure to shed compromises anti-viral immunity. J Immunol. 2008; 180:198–206. [PubMed: 18097020]

38. Karlsson M, Linton L, Lampinen M, Karlén P, Glise H, Befrits R, Janczewska I, Carlson M, Winqvist O, Eberhardson M. Naive T cells correlate with mucosal healing in patients with inflammatory bowel disease. Scand J Gastroenterol. 2014; 49:66–74. [PubMed: 24188321]

39. Dunne JV, van Eeden SF, Keen KJ. L-selectin and skin damage in systemic sclerosis. PLoS One. 2012; 7:e44814. [PubMed: 23028631]

40. Blanco P, Pitard V, Viallard JF, Taupin JL, Pellegrin JL, Moreau JF. Increase in activated CD8+ T lymphocytes expressing perforin and granzyme B correlates with disease activity in patients with systemic lupus erythematosus. Arthritis Rheum. 2005; 52:201–11. [PubMed: 15641052]

41. Shaabani N, Honke N, Dolff S, Görg B, Khairnar V, Merches K, Duhan V, Metzger S, Recher M, Barthuber C, Hardt C, Proksch P, Häussinger D, Witzke O, Lang PA, Lang KS. IFN-gamma licenses CD11b cells to induce progression of systemic lupus erythematosus. J Autoimmun. 2015; 62:11–21. [PubMed: 26094774]

42. Iwamoto T, Suto A, Tanaka S, Takatori H, Suzuki K, Iwamoto I, Nakajima H. Interleukin-21-producing c-Maf-expressing CD4+ T cells induce effector CD8+ T cells and enhance autoimmune inflammation in scurfy mice. Arthritis Rheumatol. 2014; 66:2079–90. [PubMed: 24719360]
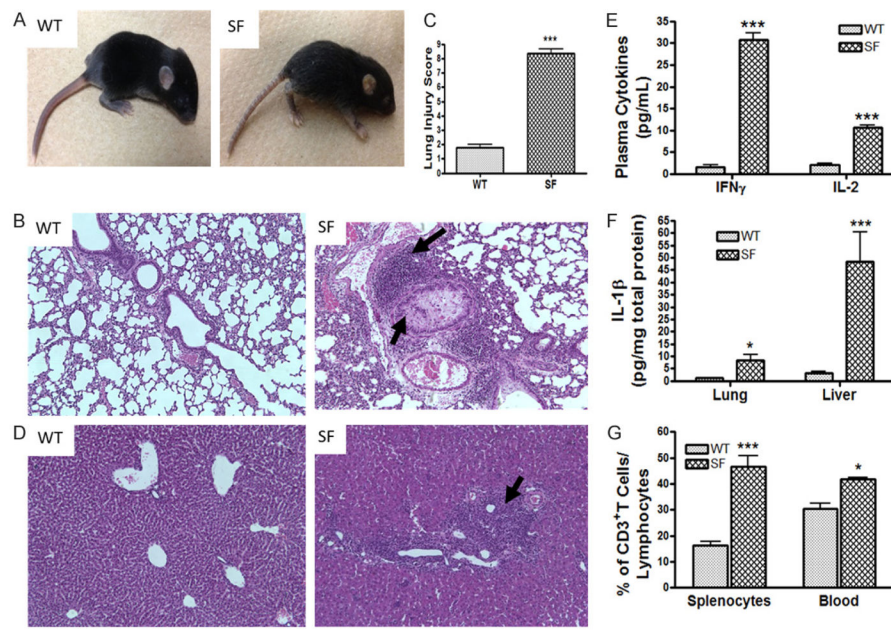
Figure 1.
Phenotypic features of scurfy mice (SF). A. A SF mouse at day 13 of life is compared to an age- matched WT mouse. It has developed scaly skin on their ears, eyes and tails, and deformed ears. B. Histology (H&E staining) of lung (100 × magnifications). Arrows indicate lymphocyte infiltrate and proteinaceous debris that filled airspaces in SF. C. Lung Injury Score (LIS) of SF compared to WT mice. D. Histology of Liver (100 × magnifications). Arrows indicate lymphocyte infiltration. E. Plasma cytokine levels of IFNγ and IL-2 in SF compared to WT. F. Inflammatory cytokine IL-1β level in lung and liver tissue lysates of SF mice compared to WT mice. G. The percentage of CD3+ T cells in the lymphocyte population from spleen and peripheral blood, comparing SF to WT mice, as analyzed by flow cytometry. All numbers represent means ± SE, *P<0.05, ***P<0.001.
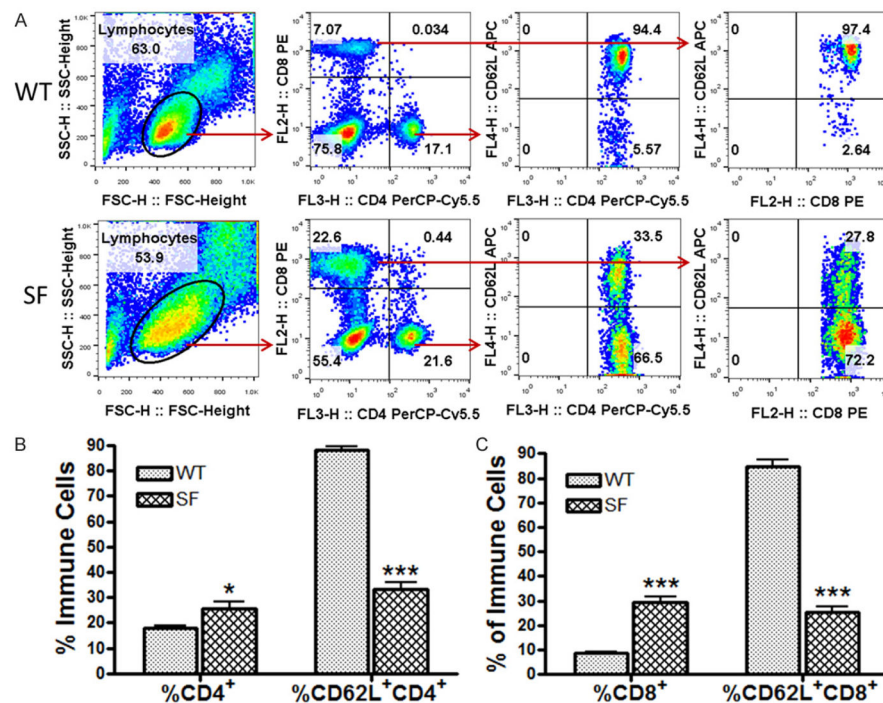
Figure 2.
A comparison of the frequencies of T cell subsets, including CD4$^+$ T cells, CD62L$^+$CD4$^+$ T cells, CD8$^+$ T cells, and CD62L$^+$CD8$^+$ T cells in the peripheral blood of SF and WT mice. (A) The definition of cell subsets and a comparison between SF and WT lymphocyte populations are shown by representative flow cytometry plots. The % of CD4$^+$ and CD8$^+$ T cells were defined among the lymphocyte population; and subsequently the % of CD62L$^+$ cells in the CD4$^+$ T cell population and in the CD8$^+$ T cell population were defined. (B, C) Bar graphs compare the % of CD4$^+$ T cell and CD62L$^+$CD4$^+$ T cell (B); CD8$^+$ T cell and CD62L$^+$CD8$^+$ T cell (C) in the peripheral blood of SF (n = 22) with WT (n = 19) mice. Numbers represent means ± SE, *P<0.05, ***P<0.001.
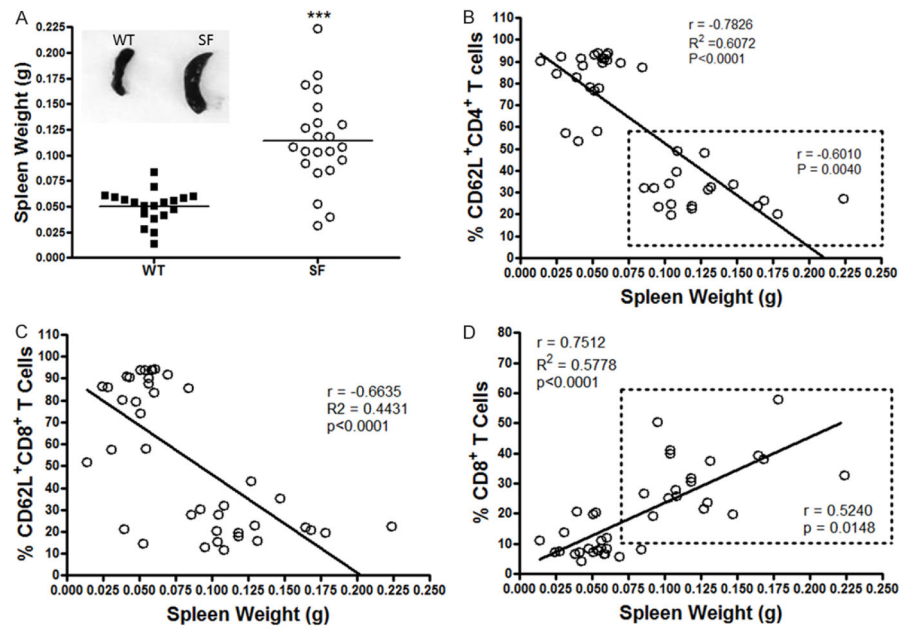
Figure 3.

Correlation between the % of T cell subsets in peripheral blood and spleen weight. A. The difference of the spleen weight of SF compared to WT mice. Each dot represents one animal, SF n = 22, WT n = 19. Mean ± SE, ***P<0.001. B. A negative correlation between the % of CD62L$^+$CD4$^+$ T cells and spleen weight was observed, r = −0.7826, P<0.0001. Shown are two separate clusters of CD62L cells: WT with a higher % CD62L$^+$CD4$^+$ T cells and SF with lower % of CD62L$^+$CD4$^+$ T cells, as shown in the dotted rectangle. We observed a significant negative correlation between the % of CD62L$^+$CD4$^+$ T cells and the weight of the spleen in SF group, r = −0.6010, P = 0.0040. C. A negative correlation between % of CD62L$^+$CD8$^+$ T cells and spleen weight was noted, when we analyzed all mice, r = −0.6635, P<0.0001. D. A positive correlation between % of CD8$^+$ T cells and splenic weight was observed (when we analyzed all mice), r = 0.7512, P<0.0001; but a positive correlation between % of CD8$^+$ T cells and splenic weight was also noted in the SF group, as shown in the dotted rectangle, r = 0.52401, P = 0.0148.
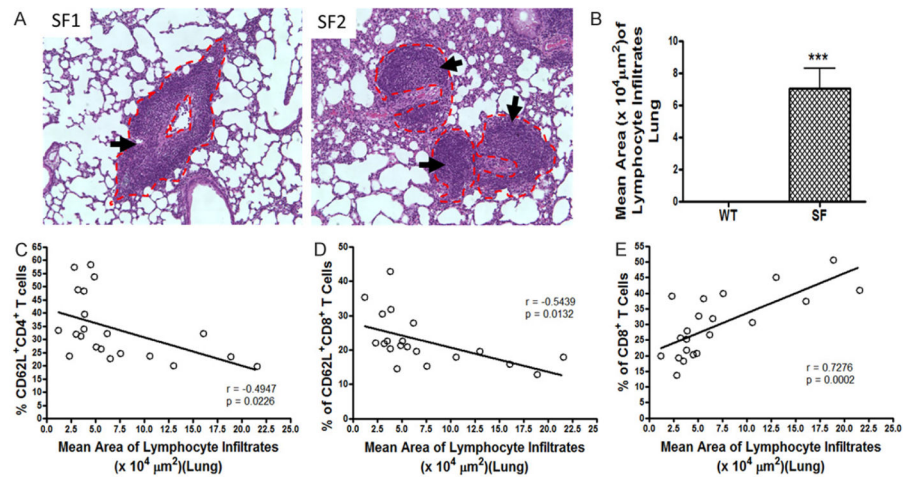
Figure 4.
Correlation between the % of T cell subsets in peripheral blood and mean area of lymphocyte infiltrates in lung. A. Histology of lungs in SF mice. Arrows indicate lymphocyte infiltrates. The dotted red lines indicate the measurement of area of lymphocyte infiltrates. The area of all lymphocyte infiltrates in 3–5 fields of each animal (100 × magnifications) was measured; and the mean area of lymphocyte infiltration was calculated. B. Bar graph indicates the mean area (μm^2) of lymphocyte infiltrates in lung of SF mice (n = 22) compared to WT mice (n = 19). The numbers represent mean ± SE, ***P<0.0001. C. A negative correlation between % of $CD62L^+CD4^+$ T cells and mean area of lymphocyte infiltrates in SF group was observed, r = –0.4947, P = 0.0226. D. A negative correlation between % of $CD62L^+CD8^+$ T cells and the mean area of lymphocyte infiltrates in SF group was noted, r = –0.5439, P = 0.0132. E. We also observed a positive correlation between % of $CD8^+$ T cells and mean area of lymphocyte infiltrates, r = 0.7276, P = 0.0002.
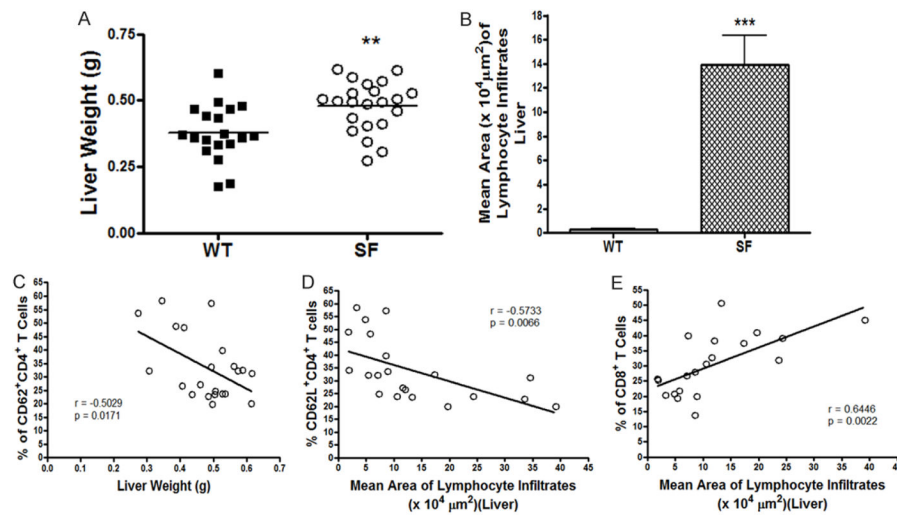
Figure 5.
Correlation between the % of T cell subsets in peripheral blood and the weight and mean area of lymphocyte infiltrates of liver. A. Figure shows a comparison of liver weight in SF mice and WT mice. **P<0.01. B. The mean area of lymphocyte infiltrates in liver of SF mice is compared with that of WT mice, as shown by means ± SE, ***P<0.0001. C. We observed a negative correlation between % of CD62L$^+$CD4$^+$ T cells and liver weight in SF group, r = −0.5029, P = 0.0171. D. There was a negative correlation between % of CD62L $^+$CD4$^+$ T cells and mean area of lymphocyte infiltrates, r = −0.5733, P = 0.0066. E. We found a positive correlation between % of CD8$^+$ T cells and mean area of lymphocyte infiltration in liver, r = 0.6446, P = 0.0022.